Initiation and Dynamics of Hemifusion in Lipid Bilayers

Guy Hed and S. A. Safran
Department of Materials and Interfaces, Weizmann Institute of Science, Rehovot 76100, Israel

ABSTRACT One approach to the understanding of fusion in cells and model membranes involves stalk formation and expansion of the hemifusion diaphragm. We predict theoretically the initiation of hemifusion by stalk expansion and the dynamics of mesoscopic hemifusion diaphragm expansion in the light of recent experiments and theory that suggested that hemifusion is driven by intramembrane tension far from the fusion zone. Our predictions include a square-root scaling of the hemifusion zone size on time as well as an estimate of the minimal tension for initiation of hemifusion. Whereas a minimal amount of pressure is evidently needed for stalk formation, it is not necessarily required for stalk expansion. The energy required for tension-induced fusion is much smaller than that required for pressure-driven fusion.

INTRODUCTION

Membrane hemifusion is a possible pathway (see Müller et al., 2002, for an alternative view) to the complete fusion of membranes (Chernomordik et al., 1995). Current theories associate the initiation of hemifusion with the formation of a contact zone between the membranes in which the two proximal monolayers are connected by a stalk-shaped neck. The stalk then expands and a region is formed (region *C* in Fig. 1), in which the two distal monolayers form a single bilayer. In general, the energetic cost of the splay of the lipid chains in the stalk prohibits its spontaneous expansion. However, the presence of additional, external forces (e.g., pressure, surface tension gradients, electrostatic effects) can lead to expansion of the stalk into a ''hemifusion region'' and to the growth of this zone. Clear evidence for the existence of these two distinct prefusion stages, stalk formation and hemifusion, was found for poly(ethylene glycol)-mediated fusion of vesicles (Lee and Lentz, 1997).

A recent theoretical paper (Safran et al., 2001) suggested that the flow of lipids from region *B* to region *A* can be caused by an increase of the surface tension in region *A* due to the presence (in that region only) of additional polymer in solution. The tension gradient between these regions induces a flow of lipids that leads to the growth of region *C*.

A different scenario, where hemifusion can be an alternative pathway to fusion, was found in influenza hemagglutinin-mediated fusion (Chernomordik et al., 1998; Leikina and Chernomordik, 2000). The initial local stalk may evolve to a fusion pore (Müller et al., 2002), or it may expand to hemifusion. In the latter case, no fusion occurs.

In this paper, we predict the dynamics of the expansion of the initial stalk and its role in the growth of a mesoscopic hemifusion diaphragm. The nucleation of a stalk by thermal fluctuations was recently shown to be thermally accessible (Kozlovsky and Kozlov, 2002; Markin and Albanes, 2002). A detailed description of the kinetics of this nucleation event (that typically describes the formation of a stalk of several nanometers in extent) is outside the scope of our work. Instead, we focus on estimates of the conditions that facilitate stalk expansion into hemifusion. We discuss the implications of our theory on biological fusion mechanisms and on in vitro experiments. In addition, we predict the growth of the hemifusion region (e.g., from nanometers to microns) as a function of time and discuss the physical parameters that can be used to control the timescale for hemifusion. This dynamic part is relevant mainly to in vitro experiments, since biological fusion events generally remain at the microscopic scale of the stalk.

If hemifusion is an intermediate state of fusion, then it is important to contrast the timescales of hemifusion diaphragm expansion and pore formation to determine the rate-limiting step. Chizmadzhev et al. (2000) predicted that pore expansion is exponential in time, with a timescale of $\eta_m/\delta p < 1$ s, where η_m is the membrane viscosity and δp is the surface tension difference (both are estimated below). However, if pore nucleation is slow enough, significant expansion of the hemifusion diaphragm can occur before pore formation. This is the case considered here, where we predict that the hemifusion diaphragm expands as the square root of time.

Our theoretical model is motivated by and consistent with the experiments described by Kuhl et al. (1996), where two bilayers supported on mica surfaces were brought into contact in the presence of a PEG-water solution. Hemifusion, which eventually extended over a distance of 50 μ, was observed in a time of $\sim$10 min, whereas the time it took the initial stalk to form was $<$3 min. This suggests that, at least in this experiment, the rate-limiting step for hemifusion is the expansion of the fusion zone, as opposed to stalk formation.

This article presents a simple theoretical model relevant to this experimental system (Kuhl et al., 1996), and predicts the time dependence of hemifusion expansion. The overall timescale we find is comparable with the measurements of Kuhl et al. (1996), although the details of the predicted temporal dependence have yet to be tested experimentally.

Submitted October 1, 2002, and accepted for publication March 21, 2003.
Address reprint requests to Guy Hed, PO Box 26, Rehovot 76100, Israel. Tel.: 972-8-9343363; Fax: 972-8-9344138; E-mail: guy.hed@weizmann.ac.il.

0006-3495/03/07/381/09 $2.00

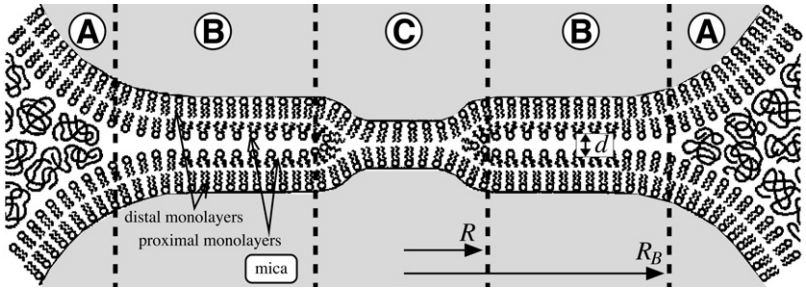

FIGURE 1 Illustration of the experimental geometry, adopted from Kuhl et al. (1996). Regions *A*, *B*, and *C* are defined in the text. R and R_B are the inner and outer radii of region *B*, respectively.

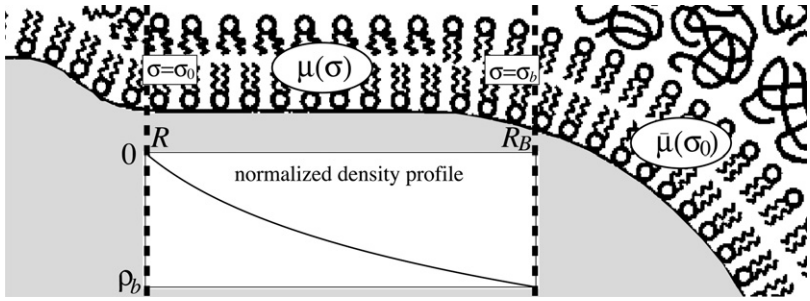

FIGURE 2 Enlargement of region *B* (between the dashed lines) shown in Fig. 1. The lipid density in region *A* is the initial density σ_0. In our model, we assume a step in the density profile, so the lipid density at R_B is $\sigma_b < \sigma_0$. At R, it is approximated by σ_0. The normalized lipid density profile $\rho = (\sigma - \sigma_0)/\sigma_0$ as a function of the radius r for $R/R_B = 0.2$ is plotted using Eq. 9. The free energy per lipid in region *B* is $\mu(\sigma)$, which is a function of the local lipid density. In region *A*, the free energy per lipid is $\bar{\mu}(\sigma_0)$ everywhere.

PHYSICAL MODEL

Our theoretical model is illustrated in Fig. 1, which is a simplification of the experimental system of Kuhl et al. (1996) wherein two bilayers deposited on mica cylinders are brought together in a solution of poly(ethylene glycol) (PEG) and water. The lipids of the distal monolayers are physisorbed on the mica; this fixes their lateral density. From here on in this paper, the term ''lipid density'' relates to the lateral density of the proximal monolayers (see Fig. 1).

We assume that the lipids are in local equilibrium, so at a particular location $\vec{r}$, the free energy per lipid (in the proximal monolayers) $\mu(\vec{r})$, does not depend on the lipid microstate, but only on the lipid density $\sigma(\vec{r})$. This assumption of local equilibrium is consistent with our results that predict an overall timescale for hemifusion expansion that is much larger than the local diffusion time of a single lipid molecule.

The experimental system we consider is macroscopically cylindrically symmetric and we therefore assume cylindrical symmetry of all the physical quantities at mesoscopic length scales. This is justified because all flows (of water and lipids) are laminar, and there are no mechanisms that might induce angular fluctuations or instabilities.

We distinguish between three regions, illustrated in Fig. 1:

Region *A*, where the distance d between the bilayers is typically much larger than the polymer correlation length ξ (Safran et al., 2001). In this region, the outer lipid monolayer is in contact with the PEG in the solution. The free energy per molecule in this region is given by $\bar{\mu}(\sigma(\vec{r}))$, and is different (in its functional form) from the free energy $\mu(\sigma)$ of the monolayer in the absence of PEG.

Region *B*, where $d \ll \xi$. For these values of d, the PEG density near the bilayers is negligible and our model assumes that there is no PEG in contact with the bilayers in this region. The free energy per lipid in this zone is $\mu(\sigma(\vec{r}))$. In addition, we assume that the distance between the mica surfaces is constant (the mica surfaces in the experiment are deformed and flattened under pressure), and that this region is ring-shaped with an outer radius R_B and an inner radius R.

Region *C*, the region where the distal bilayers are in contact.

The bilayers are Langmuir-Blodgett deposited in water, without PEG, which is added later. The energy per lipid when the monolayers are in contact with water is $\mu(\sigma)$ and the proximal monolayers are initially Langmuir-Blodgett deposited with a density σ_0 that minimizes μ. When PEG is added, it induces an effective attraction between the polar heads (Safran et al., 2001), and changes the functional form of the energy as function of the lipid density to $\bar{\mu}(\sigma)$.

The effect of lipid condensation in the presence of PEG (Bartucci et al., 1996; Maggio and Lucy, 1978; Tilcok and Fisher, 1979) has been discussed in terms of the dehydration of the bilayer by the PEG (Mishima et al., 1997). This dehydration affects the lipids in region *A* that are in microscopic proximity to the PEG, but has no effect on the lipids in region *B*. In the section ''The Role of Pressure'', we demonstrate that the osmotic pressure induced by the PEG is too small to induce hemifusion. This stands in contrast to the surface tension effects that are the main focus of our work.

If equilibrium could be reached, the lipid density in region *A* would tend to increase in the presence of PEG. However, the number of lipids in the monolayers cannot increase to any

significant degree within the timescale of the experiments, since the concentration of lipids in the bulk solution is negligible and the number of lipids that can be transported from region B to region A is much smaller than that of region A. Thus, the lipid density is unchanged and the energy per lipid in region A is now $\bar{\mu}(\sigma_0) > \mu(\sigma_0)$, with the derivative $\bar{\mu}'(\sigma_0) < 0$ due to the induced head attraction. This condensation effect thus leads to a negative tension in the proximal monolayers that ideally would cause them to contract in extent. They cannot do this without exposing the chains of the inner monolayers to the water, and this is energetically prohibitive. The outer monolayers are therefore stressed, and one way of relieving that stress is for additional lipid to enter this region; this will allow the local lipid density to increase while still covering the original area occupied by the outer monolayer.

The PEG concentration near the outer monolayers in region B is given by $c_B = c_A(d/\xi)^2$, where c_A is the PEG concentration near the outer monolayers in region A, ξ is polymer correlation length, and d is the distance between the bilayers in region B (Safran et al., 2001). Since by the definition of region B the bilayer spacing in that region is small, $d \ll \xi$, we have $c_B \ll c_A$ and the PEG concentration in region B is negligible; we thus take this concentration to be zero. The energy per lipid in region B is initially given by $\mu(\sigma_0)$, where σ_0 is the lipid density in the absence of polymer. Since the free energy per lipid, μ, is minimized when the density $\sigma = \sigma_0$ and the tension in region B initially vanishes, either expansion or compression of the lipids will increase their energy. The tension gradient between regions A (initially at negative tension) and B (initially at zero tension) induces a flow of lipids from region B to region A. Since region A is much larger than region B, we can treat it as a reservoir, and assume that even though lipid is flowing from region B to region A, the lipid density in region A is not changed from its initial value of σ_0. The system is a dynamical one, and the chemical potential (equivalent in our single-component system to the free energy per lipid, μ) is not constant in all of space at the mesoscopic scale; this results in lipid flow and dynamics. However, since local equilibrium is maintained, we must have equal chemical potentials at any given point in the system. In particular, at the boundary between regions A and B, the chemical potentials of the lipids must be equal: $\mu(\sigma_b) = \bar{\mu}(\sigma_0)$, where $\sigma_b = \sigma(R_B)$ is the lipid density at the edge of region B. We note that this equality of chemical potentials determines the lipid density at the boundary of region B, σ_b; the functional form of the two free energies $\mu(\sigma)$ and $\bar{\mu}(\sigma)$ are not the same, since in region A the lipids are in contact with polymer.

The initial lipid density in region B (σ_0, the density at which the lipids self-assemble in water in the absence of polymer) is higher than the lipid density at the AB boundary: $\sigma_0 > \sigma_b$. This inequality is a consequence of the fact that the tension at the boundary is negative, as shown in the section ''Boundary Conditions and Global Dynamics''. More intuitively, the negative tension in region A tends to pull in additional lipids from the boundary region of region B into region A as explained above. This lipid flow reduces the lipid density at the boundary $r = R_B$ from σ_0 to σ_b. In turn, the reduced lipid density at the boundary of regions A and B, ($\sigma_b < \sigma_0$) induces a flow of lipids from the rest of region B toward the boundary. This is because the minimum energy state in region B is one where $\sigma = \sigma_0 > \sigma_b$; thus lipids from the entirety of region B flow to the boundary in an attempt to restore the lipid density there to values closer to σ_0. This flow, in turn, reduces the lipid density at the boundary between regions B and C (the hemifusion region) at $r = R$, and lead to a negative tension that tends to expand region C.

At the boundary of regions B and C, the lipid density is determined by a force balance between the membrane negative tension (arising from the lipids flowing to the AB boundary) that tends to expand region C, and the force exerted by the boundary ring around region C that tends to shrink it. The main contribution to the energy of this ring is of the tilt of the lipid tails imposed by the toroidal geometry. This tilt is needed to form the three-way junction of the boundary ring cross section while avoiding an intramembrane void, which has a much higher energetic cost (Kozlovsky and Kozlov, 2002). The energetic cost of the tilt can be considered through the related intramembrane strain and the adjacent stress tensor (Hamm and Kozlov, 2000).

We assume that for $R \gg d$ the energetic cost f_t for a cross section of the BC boundary ring is independent of R. Thus, the ring energy is given by $E_r(R) = 2\pi R f_t$. The force per unit length that the ring exerts on region B of the membrane tends to shrink region C and pull region B in the $-\hat{\mathbf{r}}$ direction. This force (per unit length) is

$$\frac{1}{2\pi R}\left(-\frac{\partial E_r}{\partial R}\right)\hat{\mathbf{r}} = -\frac{f_t}{R}\hat{\mathbf{r}}, \tag{1}$$

and tends to shrink the boundary ring; that is, the expansion of region C is energetically costly. In local equilibrium, this force is balanced by the surface tension p, which may be considered as a two-dimensional lateral lipid pressure in region B of the monolayer that tends to expand the ring:

$$p(R) + \frac{f_t}{R} = 0. \tag{2}$$

Negative tension in region B tends to cause this region to contract and thus provides a force in the $\hat{\mathbf{r}}$ direction, balancing the force due to the BC boundary.

MONOLAYER DYNAMICS

In this section, we derive the dynamics that govern the expansion of the hemifusion region and predict the flow of lipids within the monolayer as a function of the lipid density and of time.

There are three local, dissipative forces that oppose any lipid motion:

- The stress, or force per unit area due to the viscosity of the water that is moved along with the lipids, is given by $\eta\partial v_w/\partial z$, where v_w is the water velocity and $\eta = 0.01$ erg s/cm^3 is the viscosity of water. The stress is of order $\eta v/d$, where v is the lipid velocity and d is the spacing between the bilayers in region B.
- The stress, or force per unit area due to the monolayer viscosity, is given by $\eta_m\nabla^2 v$, where η_m is the monolayer friction coefficient (Seifert and Langer, 1993). For a laminar flow, we estimate this stress as $\eta_m v/R_B^2$; that is, the relevant dimension is the size of region B in which there is monolayer flow.
- The stress, or force per unit area that is due to the friction between the monolayers, is given by bv, where b is the friction coefficient. This stress depends only on the motion of the outer relative to the inner monolayer where there is no flow; there is, therefore, no dependence of the length scale related to the geometry of the different regions.

The friction between a dimyristoylphosphatidylcholine (DMPC) monolayer and a supporting HTS (trichlorosilanes with hexadecyl chains) monolayer at $T = 45$°C is $b = 7 \cdot 10^6$ erg s/cm^4, whereas for a supported OTS (trichlorosilanes with octadecyl chains) monolayer the friction is $b = 2.9 \cdot 10^8$ erg s/cm^4 (Merkel et al., 1989). The experiments of Kuhl et al. (1996) were carried out at 25°C. It has been observed that the diffusion coefficient of a molecule in a DMPC monolayer increases about threefold when T is increased from 25°C to 45°C (Haibel et al., 1998; Merkel et al., 1989; Vaz et al., 1985), which suggests a corresponding decrease in b. In this work we use an estimated value of $b = 10^8$ erg s/cm^4. For DMPC bilayers at $T = 25$°C, the bilayer viscosity is $\eta_m \sim 3 \cdot 10^{-7}$ erg s/cm^2 (Merkel et al., 1989). The values relevant to the experiments of Kuhl et al. (1996) are $d = 2 \cdot 10^{-7}$ cm and $R_B = 5 \cdot 10^{-3}$ cm. With the estimates for the stress given above, we find that the frictional force due to relative motion of the two monolayers is much larger than either the lipid or water viscosity contributions to the stress. We thus neglect these latter two effects and predict the dynamics for a system where the only relevant dissipation is due to the relative friction between the monolayers.

The lipid flow is induced by the tension gradient ∇p, and is opposed by the frictional bv. The force balance equation is

$$-\nabla p - bv = 0. \tag{3}$$

In Appendix A, we derive the lipid local dynamics using Eq. 3 and the continuity equation. We consider the dynamics only to first order in the lipid density variations $\rho = (\sigma - \sigma_0)/\sigma_0$, which is known from experiments to be small. In Kuhl et al. (1996) a variation of $|\rho| \approx 0.05$ was measured.

To first order in ρ, the local dynamics has the form of a diffusion equation

$$\frac{\partial \rho}{\partial t} = \frac{\alpha}{b}\nabla^2\rho, \tag{4}$$

where $\alpha = \sigma_0^3\mu''(\sigma_0)$ is the harmonic ''spring constant'' of the monolayer. For a small density variation $|\rho| \ll 1$, the surface energy cost is $\delta g = (1/2)\alpha\rho^2$, and the related tension difference is $\delta p = \alpha\rho$. We note that the surface energy $g = \sigma\mu(\sigma)$ is the Gibbs free energy per unit area, and is different than the surface tension p, which has the thermodynamic role of the two-dimensional pressure.

We estimate α using the phenomenological form

$$\mu(\sigma) = \gamma\left(\frac{1}{\sigma} + \frac{\sigma}{\sigma_0^2}\right), \tag{5}$$

where γ is the effective surface tension of the hydrocarbon-water interface (Ben-Shaul, 1995). The second term in Eq. 5 accounts for the (electrostatic) effective headgroup repulsion, whereas the first term represents the effective hydrocarbon-water repulsion. We note that this effective repulsion is smaller than the repulsion of the bare hydrocarbon-water interface, and has been estimated as $\gamma \sim 20$ erg/cm^2 (Israelachvili, 1991).

From Eq. 5, we obtain $\alpha = 2\gamma \sim 50$ erg/cm^2. For $b = 10^8$ erg s/cm^4, the effective ''diffusion constant'' is $5 \cdot 10^{-7}$ cm^2/s. This quantity is larger than the actual, microscopic diffusion constant measured for free liquid bilayers above the gel transition, which are of the order of $10^{-8} - 10^{-7}$ cm^2/s (Haibel et al., 1998; Sonnleitner et al., 1999; Vaz et al., 1985). The Einstein relation is not applicable in our case, since the flow (which happens to scale-like diffusion) of the lipids from the high to low density regions is not due to the random motion of the molecules, but due to the tension gradient $\alpha\nabla\rho$. Indeed, for a characteristic molecular area $a = 10^{-14}$ cm^2, we find that the related energy per molecule is $\alpha a \sim 10 k_B T$.

BOUNDARY CONDITIONS AND GLOBAL DYNAMICS

The boundary conditions for the lipid density were already discussed in the ''Physical Model'' section and we review them here for convenience. The local tension equilibrium at the boundary with region A determines the local lipid density σ_b at R_B. In Appendix A we show that the tension in the monolayer is given by

$$p = \sigma^2\mu'(\sigma). \tag{6}$$

Since the tension in region A is negative, from the tension equality at the boundary we see that $p(R_B) = \sigma_b^2\mu'(\sigma_b)$ is negative. Moreover, because the function $\mu(\sigma)$ has a minimum at σ_0, it is convex in a neighborhood of σ_0. If σ_b is in that neighborhood, then the condition $\mu'(\sigma_b) < 0$ yields that $\sigma_b < \sigma_0$.

The boundary ring near the hemifusion region at R exerts a force that opposes hemifusion expansion; this is because the boundary energy of the hemifusion region is increased as this region grows. This force is locally balanced by the negative tension in region B where lipids are flowing toward region A. As lipids pass from region B to A, the lipid density in region B decreases; the tension in region B, and in particular near its boundary with region C, becomes more negative and pulls on region C, causing its expansion.

The density of lipids in region B at the boundary R is determined from the force balance Eq. 2. Using Eq. 6, we may write Eq. 2 as

$$\rho(R) = -\frac{f_t}{\alpha R}. \tag{7}$$

Before the flow begins, the initial lipid density in region B is σ_0, which implies that $\rho = 0$. For this value of the lipid density, there is zero tension in region B, the stalk does not expand, and hemifusion does not develop. Due to the tension gradient between region B and A, lipids flow out of region B and a negative tension is built up. If at a certain time the lipid density at $r = R$ is low enough so that Eq. 7 is satisfied, the stalk begins to expand.

After the flow of lipids is initiated, lipids are removed from region B as they flow toward region A and the lipid density in region B is lower than σ_0. The lipid density in region B cannot, however, be smaller than the value of σ_b, because when $\sigma = \sigma_b$ the free energies per lipid in regions A and B are equal, and the flow stops. Thus, we require $\sigma_0 \geq \sigma \geq \sigma_b$ in all of region B if there is to be flow and stalk expansion that leads to hemifusion. At an early time after the stalk formation, although the stalk does not expand, the lipid density in all of region B approaches the equilibrium density profile $\sigma(r) = \sigma_b$. Using Eq. 7, the condition for the stalk to begin to expand with a finite amount of time is:

$$-\rho_b > \frac{f_t}{\alpha R_0}, \tag{8}$$

where $\rho_b = (\sigma_b - \sigma_0)/\sigma_0$ and R_0 is the radius of the stalk. In our model, we consider the process for R much larger than the molecular size R_0 that characterizes the size of the stalk. The tilt energy f_t is in general positive. From Eqs. 6 and 8, for $R \gg R_0$ we have $|\rho(R)| \ll |\rho_b|$. Since we consider all quantities only to first order in ρ_b, we use the approximation $\rho(R) = 0$.

In Appendix B we use the integral continuity equation, which expresses the conservation of the lipid number in the system, to obtain a dynamic equation for the hemifusion radius R. In Appendix C we show that the timescale that governs the local dynamics is much faster then the rate of change of R. We use an adiabatic approximation to solve the dynamics. First, we fix R and find the asymptotic ($t \to \infty$) lipid density profile

$$\rho(r) = \rho_b\left(1 - \frac{\log(r/R_B)}{\log(R/R_B)}\right). \tag{9}$$

We use this density profile (plotted in Fig. 2 for $R/R_B = 0.2$) to obtain the dependence of the hemifusion radius R on the time t to find:

$$\frac{\alpha\rho_b}{b}t = R^2\left(\log\frac{R}{R_B} - \frac{1}{2}\right). \tag{10}$$

This predicts an approximately square root dependence of the hemifusion region size on time (with logarithmic corrections). The same temporal dependence was obtained by Kumenko et al. (1999) under the assumption of constant lateral lipid density. However, their result is quantitatively different from ours since they have considered the monolayer viscosity as the main dissipative force, whereas we have showed that it is negligible compared to the friction b.

From Eq. 10 we find that the time it takes the hemifusion region to evolve from the initial stalk radius $R = R_0 \ll R_B$ to a final radius of $R = R_B$ is $\Delta t = -bR_B^2/2\alpha\rho_b$. With $\rho_b = -0.05$ and $\alpha/b = 5 \cdot 10^{-7}$ cm^2/s, we predict that the time for expansion of the hemifusion zone to a scale of $R_B = 50$ μm is $\Delta t \approx 500$ s. This is consistent with the experiment of Kuhl et al. (1996) where a time of $\Delta t = 600$ s was measured.

The time Δt found here can also be derived (up to a numerical factor) from a simple scaling argument that does not depend on the specific details of our model. As hemifusion is initiated, the tension difference between the bulk (at R_B) and the hemifusion front (at R) is $-\alpha\rho_b$. When $R_B \gg R$, the average tension gradient is $\overline{\nabla p} \approx -\alpha\rho_b/R_B$. For a fully damped flow with a friction coefficient b, the average lipid velocity is $\bar{v} = \overline{\nabla p}/b$. The hemifusion front ($BC$ boundary) advances with the velocity $\sim\bar{v}$ of the lipids near it. The time to advance a distance of R_B with a velocity $\bar{v}$ is $R_B/\bar{v} = -bR_B^2/\alpha\rho_b$.

INITIATION OF HEMIFUSION

The change in the monolayer surface energy due to the presence of PEG in region A is $\delta g = \sigma_0(\bar{\mu}(\sigma_0) - \mu(\sigma_0))$, where $\mu(\sigma_0)$ is the free energy per lipid in the absence of PEG, and $\bar{\mu}(\sigma_0)$ is the free energy per lipid in the presence of PEG. Since we have defined σ_b by the condition $\mu(\sigma_b) = \bar{\mu}(\sigma_0)$, we can expand μ around its minimal value $\sigma = \sigma_0$, and find that to lowest order in ρ_b, the surface energy difference δg and the tension difference δp induced by the PEG are

$$\delta g = \frac{1}{2}\alpha\rho_b^2; \quad \delta p = \alpha\rho_b. \tag{11}$$

In Kuhl et al. (1996), a change of $\rho_b \approx -0.05$ in lipid density was deduced from the measured thinning of the bilayer. Using the value $\alpha = 50$ erg/cm^2, we estimate $\delta g \approx 0.06$ erg/cm^2, and $\delta p \approx 2.5$ erg/cm^2.

Initiation of stalk expansion is relevant not only to events

of mesoscopic fusion, but also to in vivo fusion events, where a fusion pore is formed soon after stalk expansion. In many cases of biological interest, the fusion process is regulated by fusion proteins that promote stalk formation and expansion. One hypothesized biomolecular mechanism that promotes expansion is the penetration of hydrophobic fusion protein domains into the membrane and its subsequent destabilization (Bentz and Mittal, 2000). The protein domains may increase the membrane surface energy by inducing an effective attraction of the hydrophobic headgroups, similar to the effect of PEG (Safran et al., 2001); they may also penetrate the membrane, increasing the intramembrane tension. Our theory suggests that the former mechanism, which works to increase in δg, may be more effective energetically than the latter, which increases δp. That is, for a given change in lipid density, ρ_b, a smaller energy is involved (Eq. 11).

SNARE (soluble *N*-ethylmaleimide-sensitive factor-attachment protein receptors) proteins that promote exocytosis in nerve synapses are thought to induce stalk expansion through a conformational change by which the proteins pull on the stalk to widen it (Scales et al., 2001). Another possible cause for stalk expansion is calcium ions induced membrane tension (Arnold, 1995). We conclude from our theory that the latter mechanism may be more effective energetically.

In the preceding section, we found that for expansion of the hemifusion region to occur, the driving force due to the negative tension in region B must be large enough to overcome the tendency of the boundary of region C to shrink. We thus deduced that the normalized lipid density at R_B must obey

$$-\rho_b > \frac{f_t}{\alpha R_0}. \tag{12}$$

From this condition, we estimate the minimum stalk radius R_0 for which the lateral tension in the monolayer can induce expansion. The energy of the lipid tails' tilt at the hemifusion front is estimated by Markin and Albanes (2002) as $f_t = 2 \cdot 10^{-6}$ erg/cm. For the values of α and ρ_b given above, we find that the mechanism described here is sufficient to cause hemifusion for $R_0 \geq 8$ nm, which is of the order of the typical radius of a thermally nucleated stalk (Yang and Huang, 2002). Note that if ρ_b vanishes (that is, no polymer is present in region A), hemifusion will not be initiated for any finite (reasonable) stalk radius.

THE ROLE OF PRESSURE

Experiments have demonstrated that hemifusion may be caused by sufficiently large normal pressure (Helm et al., 1989) or by negative pressure in the water layer (MacDonald, 1985; Yang and Huang, 2002). We shall now determine the conditions under which pressure induced in region B can in and of itself (i.e., with no surface tension effects as induced by the added polymer) cause hemifusion expansion by forcing water to flow out of the contact zone. We do this by using the simplifying assumption that the water in region B is under a constant pressure $p_w = p_n + p_o$, where p_n is the normal pressure on the bilayers and p_o is the osmotic pressure induced by the solute in the bulk. The finite thickness of the water layer in region B (whose thickness is on the order of a nanometer) is always maintained because of hydration forces: the water molecules are organized around the polar headgroups of the lipids to partially cancel their electric dipole; removing the water layer would increase the free energy because of the energetic cost of these electric dipoles whose normal components, in general, point to the same direction due to the hydrophobic nature of the lipid layer. Thus the water flow out of region B and into region A is possible only by the expansion of region C.

The energy (per unit area) difference associated with a pressure difference of p_w is $p_w d$, where d is the distance between the two proximal monolayers. This should be compared with the energy difference δg associated with the free energy gradient in the monolayer. In the experiment of Kuhl et al., (1996) that yields $p_w d \approx 0.08$ erg/cm^2, which is of the same order of δg. Nevertheless, we show below that the external normal pressure has only a minor effect on the pressure in the monolayer and on its density. We will thus show that under the experimental conditions of Kuhl et al. (1996), the external pressure is insufficient to cause hemifusion expansion.

In the experiment of Kuhl et al. (1996), the applied normal pressure is $p_n = 0.3$ atm and the osmotic pressure is $p_o \sim 0.1$ atm, so the total pressure between the bilayers is $p_w \approx 0.4$ atm. We now estimate the contribution of this pressure to the lipid density variation in the experiment. For a fluid membrane, the relation between the tension p—the two-dimensional pressure in the membrane—to the three-dimensional pressure p_w is $p_w = p/h$, where h is the thickness of the monolayer. To induce the observed density variation $\rho_b = 0.05$, the tension needed is $|p| = 2.5$ erg/cm^2. For $h = 5$ nm, the pressure required to induce such tension is 5 atm—much larger than the actual pressure in the experiment. Thus, the contribution of the normal and the osmotic pressures to the density variation is negligible compared with the surface tension effects due to the PEG-lipid interactions that result in densification of the lipids. This result underscores the point made in the preceding section: changes in the pressure are much less effective than surface energy variation for the initiation of stalk expansion.

We now estimate the pressure p_w needed to initiate hemifusion, without a lipid density gradient (that is, with $\rho_b = 0$). The radial force per unit length on the boundary at R due to the external normal pressure is

$$\frac{-1}{2\pi R}\frac{\partial(p_w V)}{\partial R} = p_w d. \tag{13}$$

From Eq. 1, the condition for spontaneous fusion is $p_w d > f_t/R_0$. For the values given above, we require $p_w \geq 10^7$ dyne/

$cm^2 = 10$ atm. Experimental results in different conditions are within that range. The pressure needed for the hemifusion of bilayers directly supported on mica (with no added polymer or other mechanisms that give rise to lipid density gradients) was found by Helm et al. (1989) to be $p_w \sim 40$ atm. Wong et al. (1999) used a surface-forces apparatus to apply pressure on DMPC bilayers supported on polymer layers. The polymer layer allowed the bilayers some lateral conformational freedom, thus permitting more freedom for the adjustment of stalk shape and size (Kozlovsky and Kozlov, 2002; Markin and Albanes, 2002). In that case, where the stalk geometry could easily adjust, the cost for forming the stalk was reduced and hemifusion was observed at a much lower pressure of $p_w = 2$ atm. In the experiment of Kuhl et al. (1996), the pressure $p_w \approx 0.4$ atm is too low to be the driving force for hemifusion.

Pressure in itself is not enough to cause hemifusion, but it is sometimes necessary. (In the experiments, it is difficult to distinguish between applied pressure and time in contact effects (T. Kuhl, private communication)). Leckband et al. (1993) showed that the amount of pressure needed for hemifusion is directly related to the lipid density near the contact area. In that experiment, two bilayers were brought into contact using a surface-forces apparatus. When Ca^{2+} ions were introduced, there was a phase separation in the bilayers. The density of lipids in the bilayer regions that were brought into contact was characterized by the hydrophobic adhesion energy. When thinner regions were brought together (characterized by adhesion energy of $E_{ad} = 3.8$ erg/cm^2), they either hemifused spontaneously or required only a small amount of pressure ($p_n \leq 1$ atm) to induce hemifusion. For denser bilayers ($E_{ad} = 0.15$ erg/cm^2), a pressure of $p_n = 4$ atm was required for hemifusion.

Yang and Huang (2002) induced negative osmotic pressure on the water layer between the bilayers by lowering the relative humidity of the environment of diphytanoyl phosphatidylcholine. At 80% humidity, the lipids were at the lamellar phase. As the relative humidity was decreased, the water was expelled from between the bilayers by the osmotic pressure and the lamella were connected by stalks, directly observed by x-ray diffraction. In this experiment, the dehydration was due to negative pressure of the water layer induced by the reduced relative humidity and not by normal pressure, but the physical effect of the two is similar.

SUMMARY

In this paper, we used a model based on lipid density gradients induced by surface energy variation that occur far from the hemifusion zone to predict the conditions for the initiation of hemifusion by stalk expansion and the dynamics of mesoscopic hemifusion. Our theory was motivated by the experiments of Kuhl et al. (1996). However, the quantitative scheme presented here can be generalized to any system of two lipid bilayers initially connected by a stalk, where a perturbation in region A, mesoscopically far from the stalk, causes tension in the membrane in that region. For example, one can apply our results to tension induced by the electrostatic interactions caused by calcium ions (Leckband et al., 1993), tension induced by laser tweezers (Bar-Ziv and Moses, 1994; Moroz et al., 1996), or the effective tension induced by the attraction of oppositely charged bilayers (Pantazatos and MacDonald, 1999).

We have compared the effect of the friction of the two monolayers, the water viscosity, and the intramonolayer viscosity on the two-dimensional lipid motion and showed that the friction dominates. Thus, the lipid dynamics depend on the friction and not on hydrodynamics. This means that the spacing between the two layers is irrelevant for the lipid dynamics.

Experiments similar to those of Kuhl et al. (1996) can test the predictions of the model for the timescales as functions of the lipid density and friction as well as the value of the driving force due to the tension induced in region A. One could vary each of the parameters ρ_b (the relative change in lipid density), α (related to the induced tension), and b (the interlayer friction) independently, and measure the ''hemifusion radius'' $R(t)$, the final radius R_B, and the time to complete the process Δt as functions of these parameters.

In particular, the friction b can be varied independently of α by changing the composition of the distal bilayers while maintaining the same composition of the proximal bilayers. The friction can be varied by varying those interactions among the chains that most directly affect the friction, such as variations of the chain length or temperature (Yoshizawa et al., 1993).

Once an empirical, temporal profile for the hemifusion expansion, $R(t)$, is measured for systems with known parameters, one can use the same experiment to estimate the effective diffusion constant for the lipid flow, α/b, for different lipid bilayers. One can easily vary the lipid density at the boundary, σ_b, by changing the polymer (or calcium ions) concentration since the density σ_b is determined by the equality of the chemical potentials of the lipids exposed to the polymer and those exposed only to the water.

The static part of our theory deals with the initial conditions required for stalk expansion. We have evaluated the necessary density variation $\rho_b = -f_t/\alpha R_0$ and demonstrated that the related surface energy $(1/2)\alpha\rho_b^2$ is much smaller then the surface tension $\alpha\rho_b$. This result is not surprising, since it is a general result of a first order expansion around an energetic minimum. Still, it does give a new insight regarding biological fusion mechanisms. It suggests that mechanisms working through the change of the surface energy δg are much more effective than mechanisms that exert force or normal pressure on the stalk.

The predicted dependence of stalk expansion on the lipid density can be tested by measuring the critical density ρ_b at which stalk expansion occurs. The results may serve to learn more about the stalk structure and energetics.

We expect that near the end of the process of hemifusion expansion, when $R(t) \approx R_B$, experimental results may differ from our predictions, since the density profile of the polymer (or calcium ions in the case of Leckband et al. (1993)) may vary in a gradual manner around R_B; in our theory we assumed a sharp (''step function'') decrease of the polymer density at R_B. We also expect a deviation from our theory when the radius $R(t)$ of the hemifusion region is close to its initial, molecular stalk radius R_0, due to microscopic details of the lipid structure in the stalk.

We distinguish between hemifusion induced by surface tension gradients, which we consider in our model, and hemifusion induced by pressure. Hemifusion may be induced by normal pressure on the bilayers (Helm et al., 1989; Wong et al., 1999) or by dehydration, which induces negative pressure in the water layer between them (Yang and Huang, 2002). We showed that this pathway to hemifusion requires much more energy (per unit area) than fusion that is induced by surface tension gradients.

We have shown that the induced pressure p_w in the experiment of Kuhl et al. (1996) cannot be the primary direct cause of hemifusion. Still, pressure does play an important role in stalk formation. It may also affect stalk expansion through its effect on the lipid tilt energy f_t and on the initial stalk radius R_0.

APPENDIX A: LOCAL LIPID DYNAMICS

We present here the full calculation of the local lipid dynamics. Note that though in our final result we leave only the terms linear in ρ, one may also calculate in the same framework the nonlinear terms in the case ρ is not small.

The force balance equation is

$$-\nabla p - bv = 0, \tag{A1}$$

and the continuity equation is

$$\frac{\partial \sigma}{\partial t} + \nabla(\sigma v) = 0. \tag{A2}$$

Writing the energy per lipid as $\mu(\sigma)$, the surface tension is

$$p = -\left.\frac{\partial(N\mu(\sigma))}{\partial A}\right|_N = \sigma^2\mu'(\sigma), \tag{A3}$$

where A is the a macroscopic area and $N = \sigma A$ is the number of lipids in this area.

From Eqs. A1, A2, and A3, we have

$$\begin{aligned} b\frac{\partial \sigma}{\partial t} &= \nabla(\sigma\nabla p) \\ &= (2\sigma^2\mu'\sigma) + \sigma^3\mu''(\sigma))\nabla^2\sigma \\ &\quad + (4\sigma\mu'(\sigma) + 5\sigma^2\mu''(\sigma) + \sigma^3\mu'''(\sigma))(\nabla\sigma)^2. \end{aligned} \tag{A4}$$

To first order in the density variation ρ, Eq. A4 has the form

$$\frac{\partial \rho}{\partial t} = \frac{\alpha}{b}\nabla^2\rho + O(\rho^2), \tag{A5}$$

where $\alpha = {\sigma_0}^3\mu''(\sigma_0)$.

APPENDIX B: GLOBAL LIPID DYNAMICS

In the section ''Boundary Conditions and Global Dynamics'', we consider the boundary conditions for the lipid density. To fully predict the dynamics of hemifusion expansion, we also need to determine the flow at the boundaries. For this we use the integral form of the continuity equation:

$$\frac{\partial}{\partial t}\int_R^{R_B} 2\pi r\,dr\,\sigma(r) = -\oint_{R_B} \sigma\vec{v}\cdot d\vec{l}. \tag{B1}$$

The left side of Eq. B1 describes the rate of change of the lipid number in region B whereas the right side gives the flow of lipids through the boundary R_B. We assume cylindrical symmetry, so $\vec{v} = v_r\hat{r}$. From Eqs. A1 and A3, we obtain

$$v_r(r) = -\frac{1}{b}(2\mu'(\sigma) + \sigma\mu''(\sigma))\sigma\frac{\partial \sigma}{\partial r}. \tag{B2}$$

We now use Eq. A5 to calculate the left side of Eq. B1:

$$\begin{aligned} \frac{\partial}{\partial t}\int_R^{R_B} 2\pi r\,dr\,\sigma(r) = 2\pi\frac{\alpha}{b}&\left(R_B\left.\frac{\partial \sigma}{\partial r}\right|_{R_B} - R\left.\frac{\partial \sigma}{\partial r}\right|_R\right) \\ &- 2\pi R\sigma(R)\frac{\partial R}{\partial t}. \end{aligned} \tag{B3}$$

If we take only terms linear in ρ, Eq. B1 gives:

$$\frac{\partial R}{\partial t} = \frac{\alpha}{b}\left(\left.\frac{R_B}{2R}\frac{\partial \rho}{\partial r}\right|_{R_B} - \left.\frac{\partial \rho}{\partial r}\right|_R\right). \tag{B4}$$

APPENDIX C: ADIABATIC SOLUTION

Equations B4 and A5 along with the boundary conditions completely determine the time evolution of the monolayers to first order in ρ. From these equations, we can calculate $R(t)$ and predict the temporal profile of hemifusion expansion. We write these two equations using dimensionless variables and scale the spatial variables so that they are of order of unity to get an estimate of the timescales. The natural spatial scale is the final size of the hemifusion region, R_B. We thus define: $x = r/R_B$, $\bar{R} = R/R_B$, and $\bar{\rho} = \rho/\rho_b$ as well as two time variables: a ''fast'' time $\tau = \alpha t/bR_B^2$ at which the local lipid flow occurs, and a ''slow'' (since ρ_b is small) time $\bar{\tau} = |\rho_b|\tau$, which is the scale over which the hemifusion region expands. Equations. B4 and A5 become

$$\frac{\partial \bar{\rho}}{\partial \tau} = \frac{\partial^2\bar{\rho}}{\partial x^2} + \frac{1}{x}\frac{\partial \bar{\rho}}{\partial x}, \tag{C1}$$

$$\frac{\partial \bar{R}}{\partial \bar{\tau}} = \left.\frac{\partial \bar{\rho}}{\partial x}\right|_{x=\bar{R}} - \frac{1}{2\bar{R}}\left.\frac{\partial \bar{\rho}}{\partial x}\right|_{x=1}. \tag{C2}$$

Since all the variables that appear on the right side of Eqs. C1 and C2 are of order unity, the units of τ and $\bar{\tau}$ suggest the timescales of the processes described by the equations. For $|\rho_b| \ll 1$ we have $\tau \gg \bar{\tau}$, which implies that we can use an adiabatic approximation: the local lipid flow occurs quickly so that the lipid density is instantaneously given by the asymptotic equilibrium solution of Eq. C1 for $\tau \to \infty$. We then use this solution to determine the slower time evolution of the hemifusion radius R from Eq. C2.

At asymptotically long times, both sides of Eq. C1 vanish. The adiabatic density profile reached is

$$\bar{\rho}(x) = 1 - \frac{\log(x)}{\log(\bar{R})}. \tag{C3}$$

Plugging this solution into Eq. C2, we obtain

$$\frac{\partial \bar{R}}{\partial \bar{\tau}} = \frac{-1}{2\bar{R}\log(\bar{R})}. \quad \text{(C4)}$$

The solution of this equation is implicitly given by

$$2\bar{\tau} = \bar{R}^2(1 - 2\log\bar{R}). \quad \text{(C5)}$$

We gratefully acknowledge useful discussions with Tonya Kuhl and Jacob Israelachvili and the support of the Israel Science Foundation and the Schmidt Minerva Center.

REFERENCES

Arnold, K. 1995. Cation induced vesicle fusion modulated by polymers and proteins. *In* Handbook of Biological Physics, Vol. 1B. R. Lipowsky, and E. Sackman, editors. Elsevier, Amsterdam.

Bar-Ziv, R., and E. Moses. 1994. Instability and ''pearling'' states produced in tubular membranes by competition of curvature and tension. *Phys. Rev. Lett.* 73:1392–1395.

Bartucci, R., G. Montesano, and L. Sportelli. 1996. Effects of poly(ethylene glycol) on neutral lipid bilayers. *Colloids Surf. A.* 115:63–71.

Ben-Shaul, A. 1995. Molecular theory of chain packing, elasticity and lipid-protein interaction in lipid bilayers. *In* Handbook of Biological Physics, Vol. 1B. R. Lipowsky, and E. Sackman, editors. Elsevier, Amsterdam.

Bentz, G., and A. Mittal. 2000. Deployment of membrane fusion protein domains during fusion. *Cell Biol. Int.* 24:819–838.

Chernomordik, L. V., A. Chanturiya, J. Green, and J. Zimmerberg. 1995. The hemifusion intermediate and its conversion to complete fusion: regulation by membrane composition. *Biophys. J.* 69:922–929.

Chernomordik, L. V., V. A. Frolov, E. Leikina, P. Bronk, and J. Zimmerberg. 1998. The pathway of membrane fusion catalyzed by influenza hemagglutinin: restriction of lipids, hemifusion, and lipidic fusion pore formation. *J. Cell Biol.* 140:1369–1382.

Chizmadzhev, Y. A., P. I. Kuzmin, D. A. Kumenko, J. Zimmerberg, and F. S. Cohen. 2000. Dynamics of fusion pores connecting membranes of different tensions. *Biophys. J.* 78:2241–2256.

Haibel, A., G. Nimtz, R. Pelster, and R. Jaggi. 1998. Translational diffusion in phospholipid bilayer membranes. *Phys. Rev. E.* 57:4838–4841.

Hamm, M., and M. M. Kozlov. 2000. Elastic energy of tilt and bending of fluid membranes. *Eur. Phys. J. E.* 3:323–335.

Helm, C. A., J. N. Israelachvili, and P. M. McGuiggan. 1989. Molecular mechanisms and forces involved in the adhesion and fusion of amphiphilic bilayers. *Science.* 246:919–922.

Israelachvili, J. 1991. Intermolecular & Surface Forces, 2nd ed. Academic Press, London. Chapter 17.

Kozlovsky, Y., and M. M. Kozlov. 2002. Stalk model of membrane fusion: solution of energy crisis. *Biophys. J.* 82:882–895.

Kuhl, T., Y. Guo, J. L. Alderfer, A. D. Berman, D. Leckband, J. Israelachvili, and S. W. Hui. 1996. Direct measurement of polyethylene glycol induced depletion attraction between lipid membranes. *Langmuir.* 12:3003–3014.

Kumenko, D. A., P. I. Kuzmin, and Y. A. Chizmadzhev. 1999. Stalk dynamics and lipid flow upon membrane hemifusion. *Biol. Membrany.* 16:472–480.

Leckband, D. E., C. A. Helm, and J. Israelachvili. 1993. Role of calcium in the adhesion and fusion of bilayers. *Biochemistry.* 32:1127–1140.

Lee, J., and B. R. Lentz. 1997. Evolution of lipidic structures during model membrane fusion and the relation of this process to cell membrane fusion. *Biochemistry.* 36:6251–6259.

Leikina, E., and L. V. Chernomordik. 2000. Reversible merger of membranes at the early stage of influenza hemagglutinin-mediated fusion. *Mol. Biol. Cell.* 11:2359–2371.

MacDonald, R. I. 1985. Membrane fusion due to dehydration by polyethylene glycol, dextran, or sucrose. *Biochemistry.* 24:4058–4066.

Maggio, B., and J. A. Lucy. 1978. Interactions of water soluble fusogens with phospholipids in monolayers. *FEBS Lett.* 94:301–304.

Markin, V. S., and J. P. Albanes. 2002. Membrane fusion: stalk model revisited. *Biophys. J.* 82:693–712.

Merkel, R., E. Sackmann, and E. Evans. 1989. Molecular friction and epitactic coupling between monolayers in supported bilayers. *J. Phys. (Paris).* 50:1535–1555.

Mishima, K., K. Satoh, and K. Suzuki. 1997. Increase in molecular order of phospholipid membranes due to osmotic stress by polyethylene glycol. *Colloid Surface B.* 10:113–117.

Moroz, J. D., P. Nelson, R. Bar-Ziv, and E. Moses. 1996. Spontaneous expulsion of giant lipid vesicles induced by laser tweezers. *Phys. Rev. Lett.* 78:386–389.

Müller, M., K. Katsov, and M. Schick. 2002. New mechanism of membrane fusion. *J. Chem. Phys.* 116:2342–2345.

Pantazatos, D. P., and R. C. MacDonald. 1999. Directly observed membrane fusion between oppositely charged phospholipid bilayers. *J. Membr. Biol.* 170:27–38.

Safran, S. A., T. L. Kuhl, and J. N. Israelachvili. 2001. Polymer-induced membrane contraction, phase separation, and fusion via Marangoni flow. *Biophys. J.* 81:659–666.

Scales, S. J., M. F. A. Finley, and R. H. Scheller. 2001. Fusion without snares? *Science.* 294:1015–1016.

Seifert, U., and S. A. Langer. 1993. Viscous modes of fluid bilayer membranes. *Europhys. Lett.* 23:71–76.

Sonnleitner, A., G. J. Schütz, and T. Schmidt. 1999. Free Brownian motion of individual lipid molecules in biomembranes. *Biophys. J.* 77:2638–2642.

Tilcok, C. P. S., and D. Fisher. 1979. Interaction of phospholipid membranes with poly(ethylene glycol). *Biochim. Biophys. Acta.* 577:53–61.

Vaz, W. L. C., M. R. Clegg, and D. Hallman. 1985. Translational diffusion of lipids in liquid crystalline phase phosphatidylcholine multibilayers. a comparison of experiment with theory. *Biochemistry.* 24:781–786.

Wong, J. Y., C. K. Park, M. Seitz, and J. Israelachvili. 1999. Polymer-cushioned bilayers. II. An investigation of interaction forces and fusion using the surface forces apparatus. *Biophys. J.* 77:1458–1468.

Yang, L., and W. Huang. 2002. Observation of a membrane fusion intermediate structure. *Science.* 297:1877–1879.

Yoshizawa, H., Y.-L. Chen, and J. Israelachvili. 1993. Fundamental mechanisms of interfacial friction. 1. Relation between adhesion and friction. *J. Phys. Chem.* 97:4128–4140.